LIMNOLOGY
and
OCEANOGRAPHY: METHODS

Limnol. Oceanogr.: Methods 10, 2012, 483–495

Quenching correction for in vivo chlorophyll fluorescence acquired by autonomous platforms: A case study with instrumented elephant seals in the Kerguelen region (Southern Ocean)

Xiaogang Xing[1,2,3,4,5], Hervé Claustre[2,3], Stéphane Blain[4,5], Fabrizio D'Ortenzio[2,3], David Antoine[2,3], Josephine Ras[2,3], and Christophe Guinet[6]*

[1]Laboratory of Physical Oceanography, Ocean University of China, Qingdao, China
[2]Centre National de la Recherche Scientifique, Unité Mixte de Recherche 7093, Laboratoire d'Océanographie de Villefranche, Villefranche-sur-Mer, France
[3]Université Pierre et Marie Curie (Paris-6), Unité Mixte de Recherche 7093, Laboratoire d'Océanographie de Villefranche, Villefranche-sur-Mer, France
[4]Centre National de la Recherche Scientifique, Unité Mixte de Recherche 7621, Laboratoire d'Océanographie Microbienne, Banyuls-sur-Mer, France
[5]Université Pierre et Marie Curie (Paris-6), Unité Mixte de Recherche 7621, Laboratoire d'Océanographie Microbienne, Banyuls-sur-Mer, France
[6]Centre National de la Recherche Scientifique, Unité Propre de Recherche 1934, Centre d'Etudes Biologiques de Chizé, Villiers en Bois, France

Abstract

As the proxy for Chlorophyll a (Chl *a*) concentration, thousands of fluorescence profiles were measured by instrumented elephant seals in the Kerguelen region (Southern Ocean). For accurate retrieval of Chl *a* concentrations acquired by in vivo fluorometer, a two-step procedure is applied: 1) A predeployment intercalibration with accurate determination by high performance liquid chromatography (HPLC) analysis, which not only calibrates fluorescence in appropriate Chl *a* concentration units, but also strongly reduces variability between fluorometers, and 2) a profile-by-profile quenching correction analysis, which effectively eliminates the fluorescence quenching issue at surface around noon, and results in consistent profiles between day and night. The quenching correction is conducted through an extrapolation of the deep fluorescence value toward surface. As proved by a validation procedure in the Western Mediterranean Sea, the correction method is practical and relatively reliable when there is no credible reference, especially for deep mixed waters, as in the Southern Ocean. Even in the shallow mixed waters, the method is also effective in reducing the influence of quenching.

It is recognized that open ocean properties, especially biological ones, are chronically undersampled. During the last decade, thanks to the emergence of sea glider and profiling float technology, the density of observations has nevertheless been drastically increased, especially for the description of temperature and salinity fields. However, most of the research conducted to date using this new technology has remained restricted to 60°N-60°S (e.g., Argo program). In order to develop observational capabilities in harsh polar conditions, the use of animals as an alternative platform has been progressively tested and proved to be efficient. This new field of biologging was made possible thanks to recent progress in microelectronics, miniaturization, and satellite telemetry. While the first objective was to provide a host of new information for biologists, the idea of simultaneously gathering oceanographic parameters has naturally emerged. A synergy between biologist's efforts to understand the marine life and physical oceanographic studies became possible in the early 2000s with the development of satellite-relay biologging devices incorporating high-accuracy oceanographic sensors. These Satellite Relay Data Loggers (SRDLs) were developed at the Sea Mammal Research Unit (SMRU-UK) and provide fundamental information not only for biologists, but also for oceanographers in the form of vertical profiles of temperature and salinity using a miniaturized conductivity-temperature-depth (CTD) cell (Fedak 2004; Charrassin et al. 2008). Animal-platform technol-

*Corresponding author: E-mail: claustre@obs-vlfr.fr

Acknowledgments

Full text given at the end of this article.

DOI 10.4319/lom.2012.10.483

ogy has thus emerged from its infancy, and it is now providing valuable standard oceanographic measurements in remote regions (Charrassin et al. 2008; Roquet et al. 2011).

The progressive miniaturization of bio-sensors now makes feasible to also document biological properties in a totally automatic and remote way. Among these biological properties, in vivo fluorescence is obviously the first candidate, as the proxy for chlorophyll *a* concentration ([Chl *a*]). Historically, it corresponds to the most recorded biological properties in the open ocean (through fluorometers interfaced with CTD sensors). The reduction in size and consumption has allowed fluorometers integration onto gliders and profiling floats (Johnson et al. 2009). As part of the "IPSOS-SEAL" (Investigation of the vulnerability of the biological Productivity of the Southern Ocean Subsystems to climate change: the Southern Elephant seal Assessment from mid to high Latitudes) project, new fluorometers have been implemented on such animals. This study deals with the development of data quality control procedures allowing, from these profiles, to retrieve Chl *a* concentration in the most accurate way.

Since its introduction in 1966 by Lorenzen, in vivo fluorescence has become a widely used and popular (rapid, cost effective, and reliable) technique to estimate Chl *a* concentration in aquatic environments. The basic principle of the "standard" fluorometry for the determination of biomass in vivo can be expressed as

$$F(\lambda_{em}) = E(\lambda_{ex})\ a^*(\lambda_{ex})\ [Chla]\ \varphi_f\ Q_a^*(\lambda_{em}) \quad (1)$$

where $F(\lambda_{em})$ (mole quanta m^{-3} s^{-1}) is the detected fluorescence intensity in the emission wavelength range (λ_{em}), $E(\lambda_{ex})$ (mole quanta m^{-2} s^{-1}) is the intensity of the excitation source at a certain wavelength (λ_{ex}), $a^*(\lambda_{ex})$ (m^2 mg Chl a^{-1}) is the chlorophyll-specific absorption coefficient at the emission wavelength (λ_{ex}), [Chl *a*] (mg m^{-3}) is the Chl *a* concentration, φ_f [mole of emitted quanta (mole absorbed quanta^{-1})] is the quantum yield for fluorescence, and $Q_a^*(\lambda_{em})$ (dimensionless) is the fluorescence intracellular re-absorption factor in the emission wavelength range (λ_{em}). The product $E(\lambda_{ex})$ $a^*(\lambda_{ex})$ [Chl *a*] reflects the amount of light absorbed by phytoplankton, $F(\lambda_{em})$ indicates the fraction that is converted to fluorescence, and $Q_a^*(\lambda_{em})$ is the fraction of that fluorescence that is not re-absorbed within the cells (Babin 2008). Considering that E is constant (delivered by a controlled artificial source) and assuming the product of a^* φ_f Q_a^* does not vary, it comes that the fluorescence signal (F) would be proportional to [Chl *a*]. This assumption allows to determine [Chl *a*] through an in vivo fluorescence signal.

However, the proportionality of [Chl *a*] and F is known to be modulated by the taxonomic composition and physiological acclimation mechanisms (essentially related to light and/or nutrient history), which both determine the variability in a^*, φ_f, as well as Q_a^* (e.g., Falkowski and Kolber 1995; Babin et al. 1996; Morrison 2003; Schallenberg et al. 2008). Babin et al. (1996) show frequency distributions for a^* and Q_a^* observed in the open ocean waters of different basins, both vary over nearly an order of magnitude. As for φ_f, it varies in a more complicated manner (Morrison 2003; Schallenberg et al. 2008). As a consequence, the fluorescence–Chl *a* relationship for a given fluorometer varies according to environmental conditions.

Among the physiological acclimation mechanisms affecting the fluorescence–Chl *a* relationship, the depression of the fluorescence signal in surface waters during daylight and especially at noon, the so-called fluorescence quenching (FQ), is one of the most obvious and ubiquitous phenomena (Marra 1997; Holm-Hansen et al. 2000; Sackmann et al. 2008; Serra et al. 2009). FQ indeed represent a collection of different photoprotective (photoacclimative) mechanisms to avoid photodamage under excessive sunlight energy (Kiefer 1973; Krause and Weis 1991; Maxwell and Johnson 2000). Undoubtedly, this phenomenon requires to be properly addressed with the aim of accurately retrieving Chl *a* concentration.

Correction methods have been proposed through the use of reliable measurements of Chl *a* concentration (Cullen and Lewis 1995; Holm-Hansen et al. 2000), or through some bio-optical parameter measurements (backscattering coefficient b_b or beam attenuation coefficient *c*) used as relative references (Sackmann et al. 2008; Behrenfeld and Boss 2006). Whereas these methods appear efficient in their particular context, they are not amenable to implementation for the FQ correction of fluorescence profile acquired without any concurrent measurement. This is the case for data autonomously acquired by elephant seals in an area (Southern Ocean) where fluorescence quenching is a recognized phenomenon (Holm-Hansen et al. 2000).

The general objective of this study is to develop data quality control procedures for the accurate retrieval of Chl *a* concentration acquired by in vivo fluorometers implemented, together with CTD sensors, on elephant seals. Given that several seals were equipped as part of an "observational network," this goal is reached in two steps. We first develop a procedure that allows an intercalibration of fluorometers before their deployment to guarantee the homogeneity of Chl *a* concentration acquired by various instrumented animals in the area of interest. Thereafter, a profile-by-profile analysis is conducted to eventually correct it in case of identification of FQ issues. This correction relies on the identification of the mixed layer depth (MLD), and the associated (and here verified) assumption that chlorophyll concentration is homogenous in the mixed layer.

Materials and procedures

Fluorometer description

The SRDL includes an Argos transmitter that provides the at sea-location, a CTD sensor head developed and built by Valeport Ltd. jointly with SMRU. It includes a Keller PA-7 pressure transducer (accuracy, ± 5 dbar) along with a custom-made temperature probe containing a platinum resistance temperature detector (resolution, ± 0.001°C; accuracy, 0.02°C), an

inductive coil for measuring conductivity (resolution, ± 0.003 mS/cm; accuracy 0.04 mS/cm, Roquet et al. 2011), and the Cyclops 7 fluorometer built by Turner Design. The entire unit, the so-called tag, is potted in polyurethane and epoxyresin, measures 105 × 10 × 40 mm and weighs 450 g in the air. The SRDL CTD-Fluo tag is pressure rated to 2000 dbar.

The Cyclops 7 is a compact cylindrical (110 × 25 mm), after removal of the end cap. It delivers a voltage output that is proportional to the Chl *a* concentration or compound of interest. For Chl *a* detection, a 460 nm excitation wavelength and a 620-715 nm fluorescence detection photodiode are used.

Calibration procedures at the BOUSSOLE site

As mentioned above, based on the assumption of linear relationship between fluorescence signal and [Chl *a*], fluorometer manufacturers generally provide calibration coefficients for each fluorometer to convert fluorescence signal into [Chl *a*]. The calibration coefficients include the offset of the instrument (the so-called dark current) and a conversion factor. Nevertheless, these calibrations are generally established for a large range of Chl *a* concentrations, generally not representative of in situ conditions (see also Xing et al. 2011). They can thus be considered only as a first guess of the actual fluorescence response to Chl *a* concentration. It is thus highly desirable to confirm or adjust through in situ calibration on natural samples.

Before their operational deployments around Kerguelen, all the fluorometers were pre–calibrated. As part of the BOUSSOLE program and associated cruises (Antoine et al. 2008) in the Ligurian Sea (Western Mediterranean), each series of tag were indeed attached to a CTD rosette generally deployed at BOUSSOLE site (7.90°E, 43.37°N). This CTD cast was also associated with fluorescence measurements thanks to a Chelsea fluorometer also attached to the CTD rosette. Water samples were taken at ~10 depths, filtered on board and immediately frozen in liquid nitrogen before being stored at –80°C back in the laboratory. High performance liquid chromatography (HPLC) analysis of filters was performed according to Ras et al. (2008) for the accurate determination of total Chl *a* (Chl *a*) and accessory pigments (other chlorophylls and carotenoids).

The in-situ calibration procedures for each tag subsequently include two steps. First, the instrumental offset (Offset, units mg m^{-3}) is detected in the profile through the fluorescence value (Fluo) in deep waters (like z > 300 m), since Chl *a* concentration is considered as null at these depths. Then, the proportional slope (Slope, dimensionless) is retrieved through a linear regression analysis without intercept (y ~ x+0):

$$[\text{Chla}] = \text{Slope} * (\text{Fluo} - \text{Offset}) \quad (2)$$

Deployment location & procedures

Southern elephant seals (*Mirounga leonina*) represent a unique opportunity for studying links between environmental variability, individual physiology, behavior, and population dynamics across a range of scales in space and time. They are long-ranging and deep-diving predators that can potentially access a wide range of geographic and oceanographic regimes in the Southern Ocean (Biuw et al. 2007; Charrassin et al. 2008). At Kerguelen Island, the elephant seals were captured, anesthetized, and equipped with a Sea Mammal research Unit Satellite Relayed data logger. They were anesthetized using a 1:1 combination of Tiletamine and Zolazepam (Zoletil 100), which was injected intra-venously (Field et al. 2002). Data loggers were glued on the head of the seals, using quick-setting epoxy (Araldite AW 2101), after cleaning the hair with acetone. The SRDL automatically measure and transmit physical and biological parameters. With these animals diving to depth and returning to surface, the sensors sample vertical profiles and data are transmitted through Argos telemetry (see Roquet et al. 2011). For energy conservation purpose, only four CTD and fluorescence profiles were sampled daily and among those only 1 of 4 are, on average, successfully transmitted. From December 2007 to October 2010 SRDL-CTD-Fluo tags were deployed on 5 occasions (FT01 to FT06) on Kerguelen Island on 26 individuals, 21 of those successfully transmitted fluorescence profiles.

Dataset characteristics

In this study, we chose the latest three deployments from Kerguelen Island, which mainly covered the Kerguelen region (45°S ~ 60°S, 50°E ~ 100°E), from Oct. 2009 to Jan. 2011. The deployment numbers are referred as FT03, FT04, and FT06, respectively, and corresponding to 15 successfully equipped elephant seals. These deployments were chosen because at-sea predeployment tests were conducted during the BOUSSOLE campaign on these SRDL-CTD-Fluo tags, which was not the case for FT01 and FT02. Each deployment includes several instrumented elephant seals (which are distinguished by the tag number, like FT03-79682). The basic information for each tag is shown in Table 1.

For a typical measurement tag integrating the GPS, CTD sensor and fluorometer, the basic dataset includes the geographic location information (date, time, longitude, and latitude) together with the physical variables (temperature, salinity, pressure), and Chl *a* fluorescence. Fluorescence was monitored continuously from 175 to 5 m during the ascending phase of a dive. A fluorescence reading acquisition took place every 2 s. The profile data were pre-processed on board with a 10 m vertical resolution bins (from 5 m, 15 m, up to 175 m). For the average value of fluorescence reading were calculated for each 10 m bin. As the ascent speed of an elephant seal is about 1.5 m/s about 6 to 7 reading were collected and averaged for each bin.

Based on the sampling time, the dataset can be divided into two subsets, the day and night profiles, through the calculation of local sunrise and sunset time. For the deployment FT03 and FT06, the observations were carried out from austral spring to summer, with a longer daytime and shorter nighttime. Consequently, day profiles are denser than night ones (Table 1). For the FT04, it is the reverse as sampling periods

Table 1. The basic information of deployment and dataset.

Deployment	Tag No.	Start date	End date	All profiles	Day profiles	Night profiles
FT03	FT03-79682	20 Oct 2009	3 Jan 2010	134	77	57
	FT03-79683	21 Oct 2009	9 Jan 2010	156	102	54
	FT03-86364	19 Oct 2009	8 Jan 2010	157	115	42
	FT03-86366	16 Oct 2009	27 Dec 2009	141	89	52
	FT03-86367	23 Oct 2009	17 Jan 2010	169	114	55
FT04	FT04-49771	18 Feb 2010	27 Jun 2010	125	1	124
	FT04-49772	20 Feb 2010	26 Feb 2010	6	0	6
	FT04-49773	10 Mar 2010	14 Jun 2010	113	0	113
	FT04-49774	19 Feb 2010	28 Jun 2010	128	0	128
	FT04-49775	10 Mar 2010	22 May 2010	51	0	51
FT06	FT06-72968	9 Sep 2010	24 Nov 2010	140	68	72
	FT06-73000	4 Nov 2010	9 Jan 2011	120	101	19
	FT06-73001	21 Oct 2010	11 Jan 2011	164	108	56
	FT06-73052	26 Nov 2010	30 Dec 2010	136	88	48
	FT06-73053	9 Dec 2010	13 Jan 2011	154	128	26
Total				1894	991	903

were from austral autumn to winter. Therefore most of the profiles were acquired at night.

Determination of mixed layer depth

The mixed layer depth (MLD) is determined from the density profile. With respect to the vertical resolution of our data, the surface reference value is set at 15 m to avoid any influence of diurnal cycle in this estimation. The MLD is subsequently defined at the deepest depth where the density increase with respect to the surface value remains less than 0.03 kg m^{-3} (de Boyer Montégut et al. 2004). Such a definition supposes that the MLD is always deeper than or equal to 15 m. If the density increase from the surface reference to 175 m (deepest sampled depth) remains inferior to 0.03 kg m^{-3}, the MLD is considered to be deeper than 175 m. In such cases, the MLD is arbitrarily set to 180 m.

Assessment

Cross calibration of fluorometers

An example of in-situ calibration of the five tags of the FT04 deployment is presented in Fig. 1. It was performed as part of the BOUSSOLE cruise of 9 Dec 2009. The raw fluorescence profiles of the five tags (Fig. 1a) display an overall similar shape: increase from the surface to ~40 m where a Deep Chlorophyll maximum (DCM) develops, and then decrease from the DCM to 80 m where fluorescence returns to a background value. This value remains the same down to 400 m.

Second order differences between fluorometers are nevertheless recorded. They can be easily identified at the DCM level where the factory-calibrated values range from 0.60 to 0.93 mg m^{-3} or at depth where these values range from 0.22 to 0.33 mg m^{-3}. Owing to lack of quality control in the factory calibration process, this mismatch between factory-calibrated fluorometers illustrates the needs for an additional cross calibration.

The Offset for each tag was first calculated, through the removal from all profiles of the median value below 200 m. A linear regression was thereafter performed between Offset-corrected fluorescence and HPLC [Chl *a*] (Fig. 1b). This operation results in different Slopes for fluorometers, which cover a rather wide range, from 0.56 to 1.14 (see in Table 2).

The final calibrated profiles (Fig. 1c) agree well with each other. As a summary, such a procedure has the advantage to not only calibrate fluorescence in appropriate Chl *a* concentration units, but also to strongly reduce variability.

Initial observations of quenching

The KEOPS cruise (Blain et al. 2008), which took place in 2005 in the same sea area (Kerguelen region) as the one investigated by elephant seals, provides first examples to highlight surface fluorescence quenching at noon. Figure 2 presents the results from two stations (one sampled at night in Fig. 2a; the other at daytime in Fig. 2b) where fluorescence profiles as well as water samples for subsequent HPLC analysis (Uitz et al. 2009) were simultaneously acquired. Both HPLC Chl *a* and fluorescence profiles are almost uniform in the mixed layer at night. By contrast, fluorescence displays a significant surface depression at noon with respect to the corresponding Chl *a* profile (also see Marra 1997; Sackmann et al. 2008).

Figure 3 shows three representative situations of hydrological conditions and associated Chl *a*–calibrated profiles recorded by elephant seals. On each panel a typical pair of day and night profiles (observed within less than 24 h) is reported together with their corresponding MLDs. For the night profiles, the fluorescence always displays a quasi-uniform distribution in the upper part of the mixed layer. At the basis of the mixed layer, a weak fluorescence decrease with depth is sometimes recorded (e.g., Fig. 3b). Below the MLD, the profile generally exhibits two main different patterns: (1) the presence of

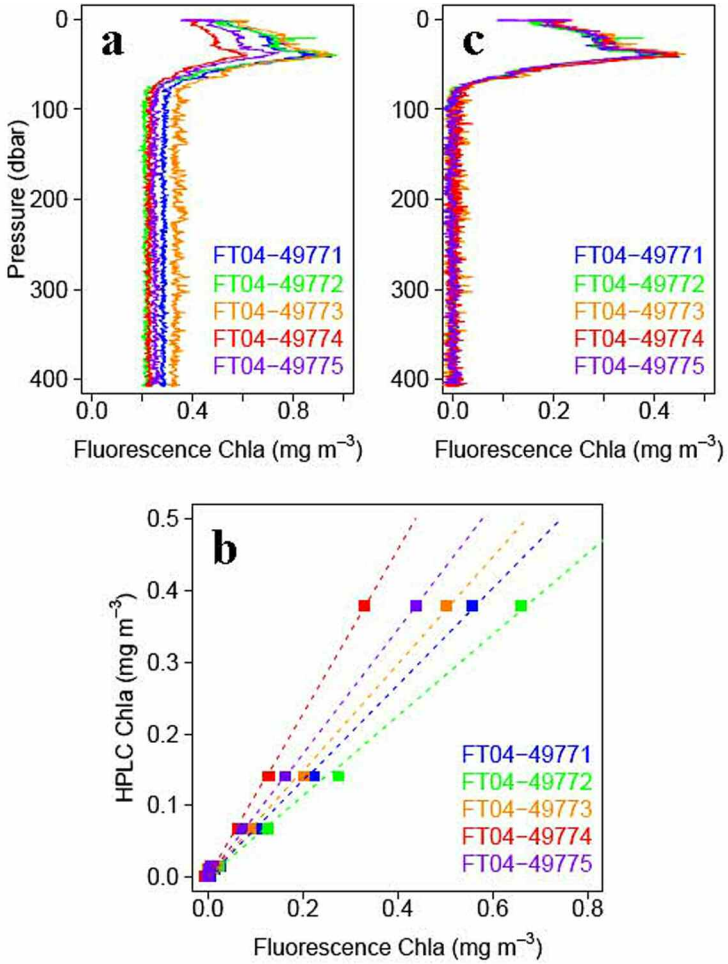

Fig. 1. The cross-calibration procedures of tag fluorometers at BOUSSOLE site (Western Mediterranean Sea, 7.9°E, 43.37°N). Fig. 1a shows the raw (uncalibrated) fluorescence profiles of five tags. Fig. 1b shows the linear regression analysis between fluorescence and HPLC Chl *a* concentration. Fig. 1c shows the calibrated fluorescence profiles.

Table 2. The cross-calibration results at BOUSSOLE site.

Deployment	Tag No.	Calibration date	Offset	Slope
FT03	FT03-79682	16-17 Jul 2009	0.17	0.62
	FT03-79683		0.24	0.57
	FT03-86364		0.16	0.70
	FT03-86366		0.20	0.28
	FT03-86367		0.28	0.59
FT04	FT04-49771	9 Dec 2009	0.28	0.67
	FT04-49772		0.22	0.56
	FT04-49773		0.33	0.74
	FT04-49774		0.23	1.14
	FT04-49775		0.25	0.86
FT06	FT06-72968	11-12 Jun 2010	0.17	0.65
	FT06-73000		0.31	1.23
	FT06-73001		0.26	1.07
	FT06-73052		0.24	1.06
	FT06-73053		0.20	0.91

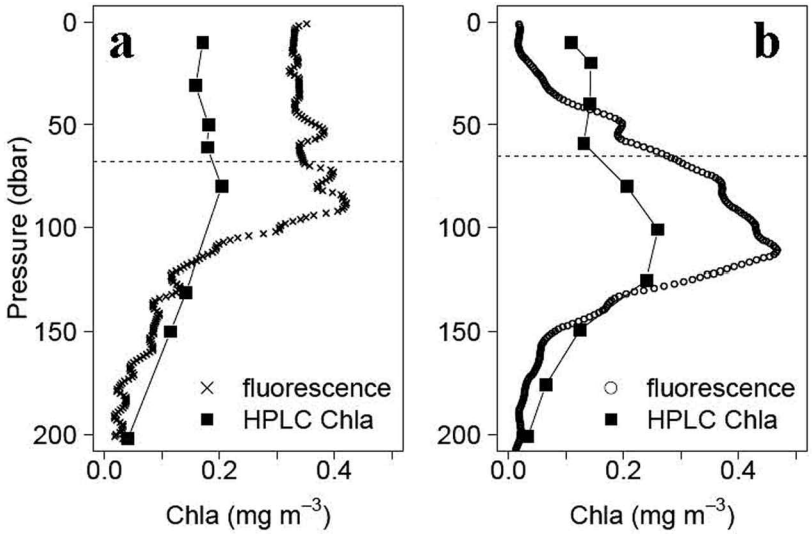

Fig. 2. Two suites of profiles, including the fluorescence and HPLC Chl *a* concentration, observed during KEOPS cruise. The profiles in Fig. 2a were measured east of the Kerguelen Plateau (Station C11, 78.002°E, 51.647°S) at night (2H30 Local time, 28 Jan 2005), and the ones in Fig. 2b were observed nearby (Station B11, 76.999°E, 50.498°S) at noon (13H30 Local time, 29 Jan 2005).

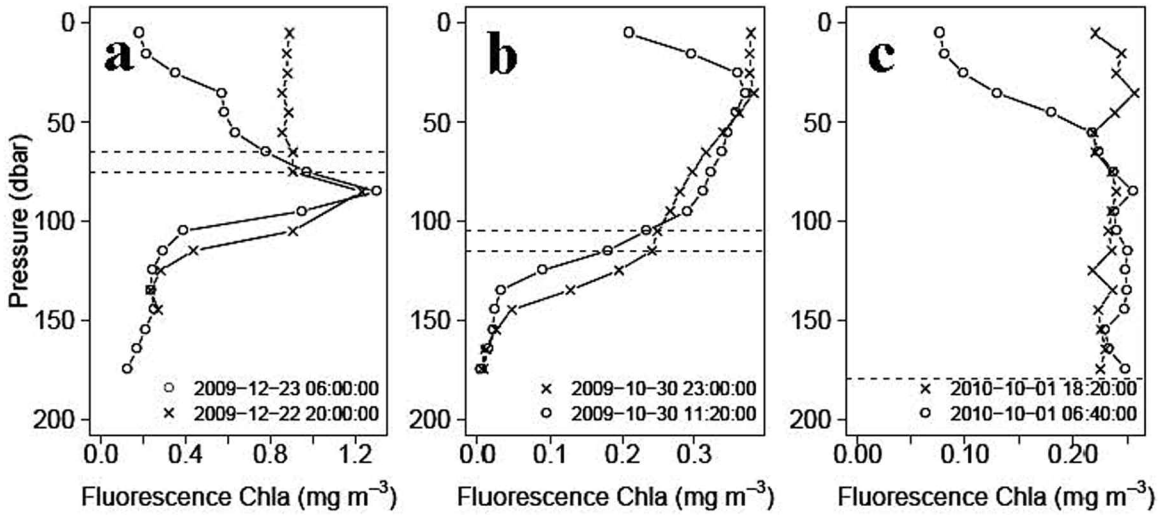

Fig. 3. Three day-night fluorescence profile pairs measured by instrumented elephant seals in the Kerguelen region (Southern Ocean). The dash lines are determined mixed layer depths. Fig. 3a shows the two profiles captured at 20H00 (GMT) 22 Dec and 6H00 (GMT) 23 Dec 2009, by the tag "FT03-79683." Fig. 3b shows the two profiles captured at 11H20 (GMT) and 23H00 (GMT) 30 Oct2009, by the tag "FT03-79682." Fig. 3c shows the two profiles captured at 06H40 (GMT) and 18H20 (GMT) 01 Oct 2010, by the tag "FT06-72968." All the "day profiles" are plotted as "o," and the night ones as "x."

a deep chlorophyll maximum (DCM), generally associated with rather shallow mixed layer (Fig. 3a); (2) a sharp decrease in fluorescence generally associated with deeper mixed layer (Fig. 3b). With MLDs deeper than 175 m, the fluorometer records a homogenous profile (Fig. 3c). By contrast and as a consequence of FQ, a clear fluorescence depression is observed toward the surface for the day profiles. Below this layer affected by quenching, the fluorescence profile remains mostly identical to its night-time analogous. This is exemplified in Fig. 3b below the 50 m depth. Furthermore, for a day profile, it appears that the depth where the quenching vanishes actually corresponds to the depth of maximal fluorescence within the mixed layer, hereafter referred to MaxFluo.

To verify this observation, which will subsequently be used for the development of a quenching correction scheme, we analyze all 588 (day-night) profile pairs acquired by elephant seals in the Kerguelen region, in FT03, FT04, and FT06 deployments. Because the quenching only appears at daytime, the night profiles are taken as the reference. For each pair, we compare the ratio of day to night values at the same depth in the mixed

layer. For highlighting the significance of MaxFluo in this quenching correction, the mixed layer is divided into two layers: the "surface" layer [between surface and the depth of MaxFluo ($z_{MaxFluo}$)] and the "deep" layer (between $z_{MaxFluo}$ and MLD). The statistical results of day/night ratios within both layers are plotted in Fig. 4. In the surface layer, the ratio distribution clearly exemplified the fluorescence quenching (a majority of values are lower than one). In the deep layer, the ratio distribution does not highlight any day-time variations for Chl *a* calibrated fluorescence (the distribution is centered about one).

Rationale of the correction method

From the above observations, it appears that the daytime fluorescence maximum, and its depth within MLD (MaxFluo and $z_{MaxFluo}$) is a good proxy to identify the thickness of the layer potentially affected by quenching. We subsequently propose to extrapolate the MaxFluo value toward the surface as a way to correct for this quenching effect. Such a correction relies on two assumptions. (1) The Chl *a* concentration is uniform or quasi-uniform in the surface layer. (2) The quenching processes do not affect the depths below the $z_{MaxFluo}$. Both assumptions are realistic given the rather deep mixed layers, which prevail in the studied area. The analysis of the MLDs recorded for the whole dataset (1841 profiles) indeed indicates that more than 80% profiles have deep MLDs (≥ 45 m), the MLDs of about 50% profiles are equal to or larger than 75 m, and for about 10% profiles, the MLDs are even undetectable (deeper than the maximal observation depth, 175 m).

For a shallow mixed layer (e.g., Fig. 3a), the FQ could still contaminate the fluorescence profile below the MLD. But even under such conditions, the quenching correction through MaxFluo will effectively reduce FQ influence. This point will be further addressed in the validation part.

Validation of the method with HPLC

To validate the quenching correction method, we used the BOUSSOLE dataset in the period of 2003-2007. This dataset encompasses 75 profiles acquired around noon, including fluorescence recorded by a Chelsea fluorometer equipped on the CTD rosette from surface down to 500 m depth, and [Chl *a*] at discrete depths quantified by HPLC. It should be noted that, contrarily to the Kerguelen region, only few profiles were characterized by significantly deep mixed layers (17 profiles with MLD ≥ 40 m). Nevertheless this dataset still remains appropriate to test the effectiveness of the proposed quenching correction method.

All fluorescence profiles were first corrected for their deep offset by the removal of the median value below 200 m (similar correction as the one described in "cross-calibration of fluorometers). Second, the averaged fluorescence data were chosen at the same discrete depths of water sampling as those of HPLC Chl *a* determination. Then, the quenching method using the MaxFluo within MLD was applied to correct the fluorescence profiles at surface (Fig. 5a and 5b). Figure 5a shows the scatter plots of fluorescence versus HPLC [Chl *a*] with the depths deeper than $z_{MaxFluo}$ for all 75 profiles, these points are used for a linear regression analysis (black line) to intercalibrate the fluorescence Chl *a* with HPLC determinations. The regressed intercalibration equation is obtained as:

$$[\text{Chl}a] = 2.25\ \text{Fluo}\ (r^2 = 0.86,\ n = 591) \qquad (3)$$

Here, two statistical parameters are introduced to quantify the effectiveness of the method, RMSE (Root Mean Square Error) and MAPE (Mean Absolute Percentage Error), defined as:

$$\text{RMSE} = \sqrt{\frac{\sum_{n=1}^{N}(A_n - P_n)^2}{N}};\ \text{MAPE} = \frac{1}{N}\sum_{n=1}^{N}\left|\frac{A_n - P_n}{A_n}\right|$$

The A_n is the actual value, and P_n is the predicted value. RMSE represents the absolute deviation, while MAPE denotes the relative error.

Figure 5b shows the scatter plot of fluorescence versus HPLC [Chl *a*] with the depths shallower than $z_{MaxFluo}$, these points are used for validation of quenching correction method. The red points are uncorrected fluorescence versus HPLC [Chl *a*], and the blue points are corrected ones versus

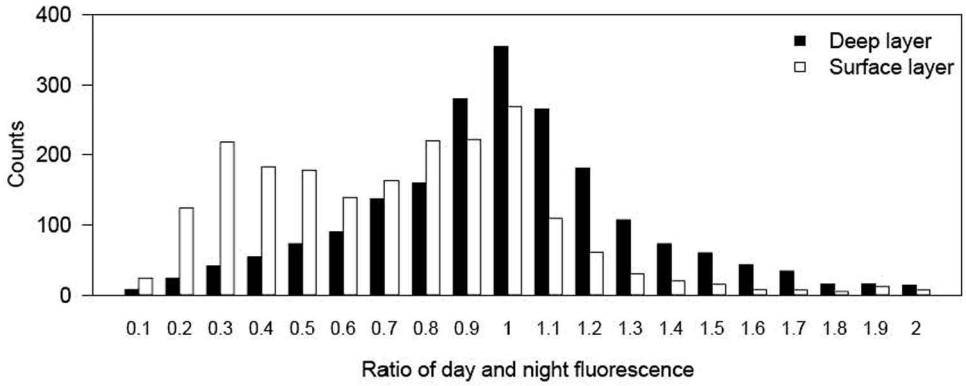

Fig. 4. The statistical histogram of the ratio of day and night fluorescence values in the mixed layer, for 588 days-night profile pairs, acquired by elephant seals in the Kerguelen region. The white columns represent the ratio counts in the "surface" layer (between surface and $z_{MaxFluo}$), and the black columns represent the ratio counts in the "deep" layer (between $z_{MaxFluo}$ and MLD).

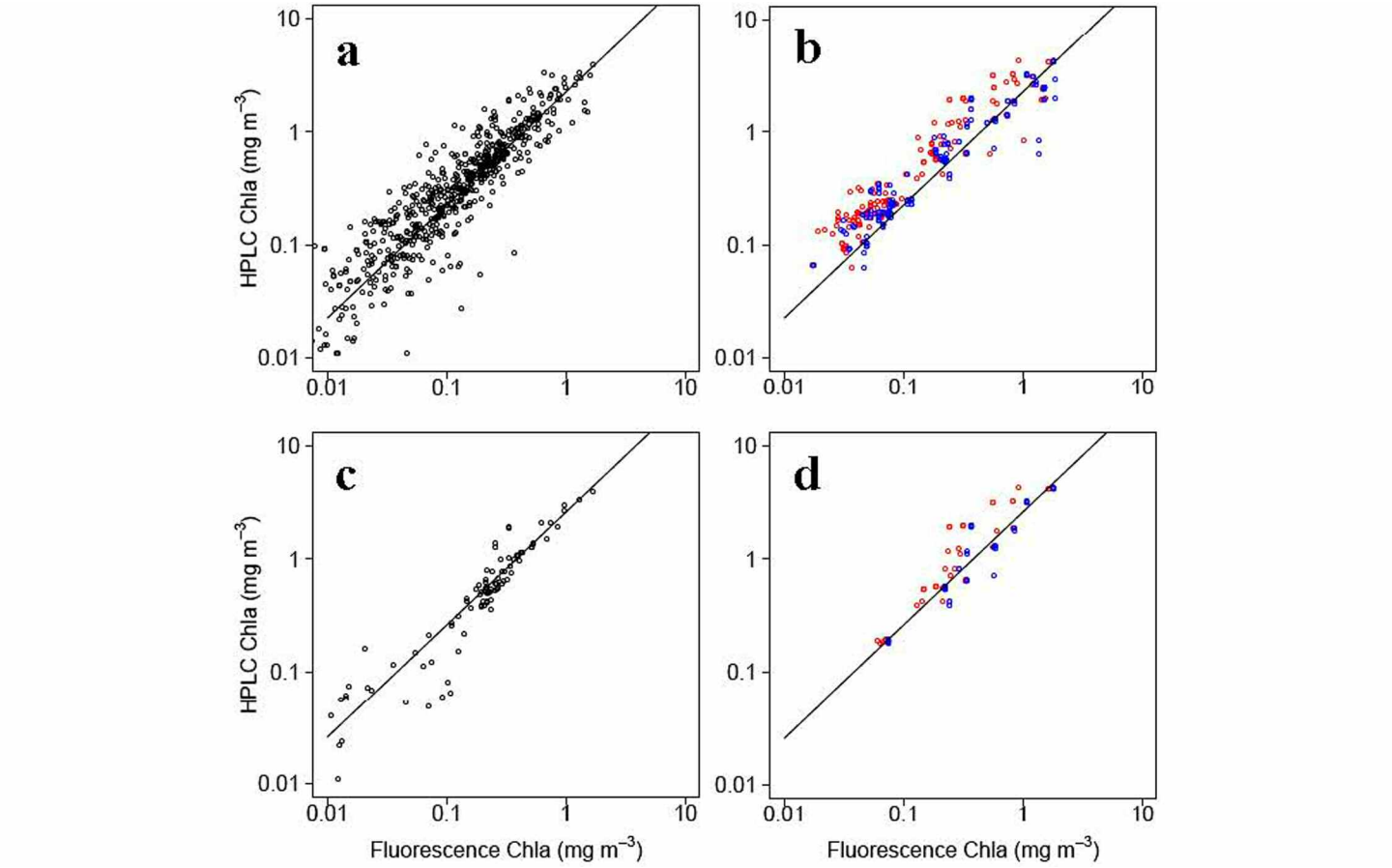

Fig. 5. The validation procedures at BOUSSOLE site. Fig. 5a shows the scatter plots of fluorescence versus HPLC [Chl *a*] with the depths deeper than $z_{MaxFluo}$ for all 75 profiles (BOUSSOLE 2003-2007), these points are used for a linear regression analysis (black line) to intercalibrate the fluorescence Chl *a* with HPLC determinations. Fig. 5b shows the scatter plot of fluorescence versus HPLC [Chl *a*] with the depths shallower than $z_{MaxFluo}$ for all 75 profiles; these points are used for validation of quenching correction method. The red points are uncorrected fluorescence versus HPLC [Chl *a*], and the blue points are corrected ones versus HPLC values. Fig. 5c and 5d show a similar scatter plot to Fig. 5a and 5b, but only for the profiles with deep mixed layers (MLD ≥ 40 m).

HPLC values. Through this regressed relation, all fluorescence values above MaxFluo (both uncorrected and corrected values) are converted into Chl *a* concentrations as the predicted values. The corresponding HPLC Chl *a* represents the actual value. The comparison between both Chl *a* estimated indicates that the corrected fluorescence Chl *a* has much less error (RMSE = 0.12 mg m^{-3}; MAPE = 29%; n = 158) than the uncorrected one (RMSE = 2.35 mg m^{-3}; MAPE = 39%; n = 158).

Considering deep mixed waters prevailing in the Southern Ocean, the same analysis is performed with a subset of the BOUSSOLE dataset selecting those 17 profiles for which MLD ≥ 40 m. Similar results are obtained (Fig. 5c and 5d), and the regression line remains basically unchanged as before with,

$$[\text{Chla}] = 2.60\ \text{Fluo}\ (r^2 = 0.95,\ n = 94) \qquad (4)$$

Again the quenching-corrected Chla fluorescence has much less error (RMSE = 0.28 mg m^{-3}, MAPE = 23%; n = 39) than the uncorrected one (RMSE = 2.36 mg m^{-3}; MAPE = 27%; n = 39).

The present validation exercise is admittedly not performed in the same area and time period than that of measurement by instrumented elephant seals. It nevertheless demonstrates that the quenching correction here proposed is quite efficient to reduce the influence of surface FQ for the accurate retrieval of [Chl *a*], even for those situations with a rather shallow mixed layer.

Application to the dataset

In Fig. 3, the day-night profile pairs were used to highlight the rather widespread quenching-induced discrepancies between day and night fluorescence profiles acquired by elephant seals in the Kerguelen region. Thus, an improvement in matching of the retrieved [Chl *a*] between day and night situations is expected after the application of the quenching correction method. The performance of quenching correction for the elephant seals dataset is shown through Figs. 6 and 7.

Figure 6a shows the plot of day versus night fluorescence [Chl *a*] in the "deep" layer (i.e., below $z_{MaxFluo}$). As expected from the frequency distribution of the ratio (Fig. 4), both values match well (close to 1:1 line). Correspondingly, Fig. 6b, which shows the same type of plot for the "surface" layer (i.e., above $z_{MaxFluo}$), clearly highlights the importance of the quenching issue (red points) and the effectiveness of the quenching correction (blue points) with the disappearance of day-night differences (all corrected data become aligned along the 1 to 1 lines).

Through the analysis of a time series of fluorescence profiles acquired in a specific area, the improvement of surface [Chl *a*] retrieval can be more explicitly pointed out (Fig. 7). An elephant seal equipped with the tag FT06-72968 acquired the time series analyzed here. From 9 Sep to 29 Oct 2009, this seal always stayed near the Kerguelen Plateau, off the Kerguelen Island coast (Fig. 7a). It captured 86 valid fluorescence profiles, including 41 days profiles and 45 night ones. A series of very deep MLDs were derived, with 76 MLDs over the maximal observation depth (> 175 m). The minimum recorded MLD

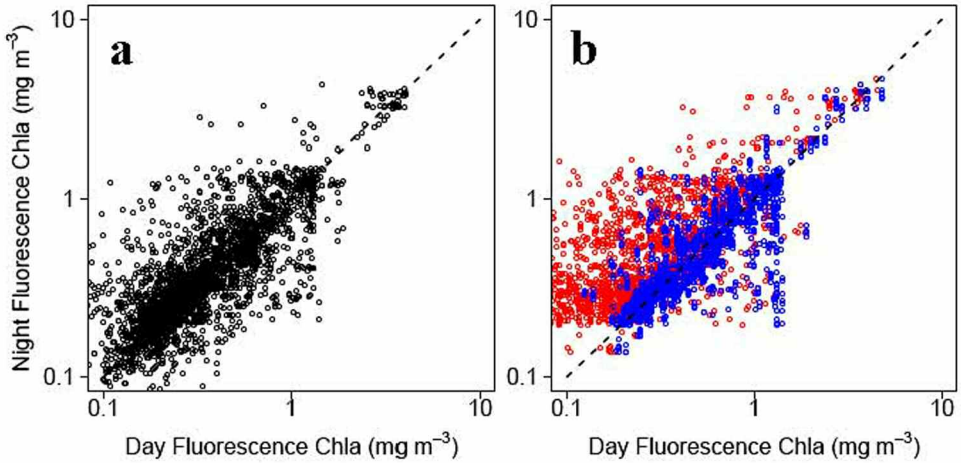

Fig. 6. The scatter plot of day versus night fluorescence values at the same depth in the mixed layer, for 588 days-night profile pairs, acquired by elephant seals in the Kerguelen region. The dash lines are 1:1 lines. Fig. 6a shows all the points in the "deep" layer (between $z_{MaxFluo}$ and MLD). Fig. 6b shows the points in the "surface" layer (between surface and $z_{MaxFluo}$), including the uncorrected (in red) and quenching-corrected points (in blue).

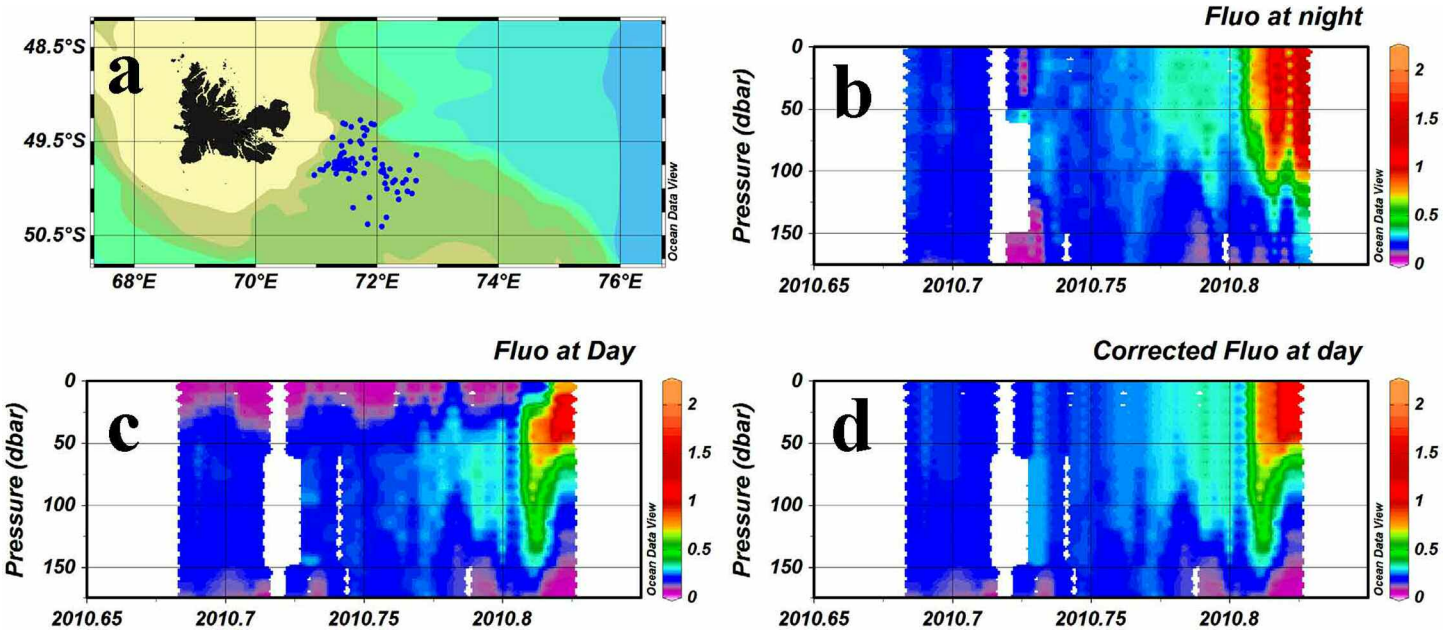

Fig. 7. A successive time series of 86 fluorescence profiles captured by the tag "FT06-72968," from 9 Sep to 29 Oct. 2009 at the Kerguelen Plateau. Fig. 7a shows the location information of the profiles. Fig. 7b shows the time series consists of 45 night profiles; Fig. 7c shows the time series consists of 41 days profiles; and Fig. 7d shows the time series consists of 41 quenching-corrected day profiles.

was 55 m.

During the observation period, fluorescence [Chl *a*] varied from 0.001 at depth (175 m) to 1.7 mg m^{-3}. The comparative analysis between day and night sections highlights an obvious FQ-related discrepancy at surface (Fig. 7b and c). Almost all the night profiles present similar characteristics, fluorescence [Chl *a*] were homogenous in the mixed layer, and there was not any quenching-induced depression at the surface. When below the mixed layer, fluorescence [Chl *a*] decreased sharply with depth (Fig. 7b). In contrast, for all the day profiles, varying degrees of FQ-issue were observed at the surface, resulting in the maximal fluorescence signal developing in the "deep" layer (Fig. 7c). Below 35 m, the quenching effect disappears so that day and night sections become coherent. Thus as expected, after applying the quenching correction procedures, the day and night sections basically show analogous profile pattern and trend (Fig. 7d).

Discussion

With the progressive generalization of the acquisition of biological variables through autonomous platforms (also including gliders and floats), very soon the oceanographic community will have to deal with the management of massive data sets (Claustre et al. 2010). Whereas the present study only deals with the analysis (and the correction) of Chl *a* fluorescence data gathered by elephant seals, the proposed method and the subsequent discussion can thus be enlarged to the broader context of autonomous platforms.

For these future large datasets of biological variables to be scientifically useful, they should be interoperable and coherent between themselves. This is an essential prerequisite because one of the ultimate goals of these new developments is to generate, over the long term, high quality datasets from which trends of climatic relevance could be eventually extracted. In this context, Chl *a* fluorescence appears as a very interesting property to be measured because it is cost effective and can be easily implemented on a variety of platforms. However, fluorescence is only a proxy of Chl *a* concentration, the most basic biological variable that we are looking for, and measuring it through remote platforms is not trivial and is associated with its own peculiarities and issues. New procedures have thus to be developed for guaranteeing the quality of the data.

The pertinence and the durability of an initial (factory or homemade) calibration of the fluorometer over its lifetime (actually over the platform duration) is a first critical issue. This is especially the case when the platforms are lost (most of the time for floats, more often for animals) so that post-calibrations are not possible. The predeployment calibrations therefore need to be trusted; this corresponds to the situation analyzed in this study. Even if we performed careful post-calibration of fluorometers using up-to-date measurement of Chl *a* concentration (HPLC in the present study), admittedly we have no way to argue this calibration was valid over the whole period of acquisition. Our pre-calibration is, of course, relevant to the Mediterranean waters at the given period of the calibration. To what extent it is relevant to Southern Ocean waters with different phytoplankton populations and associated different forcing (light and nutrient) cannot be addressed here. Nevertheless we consider that the HPLC calibration of the fluorometers remains the best that can be done in the present circumstances (i.e., no possibility to calibrate the fluorometer on site, but just before the deployment). This calibration definitively performs better than the factory one (see also below).

For other platforms than elephant seals (e.g., floats) where the implementation of radiometers is possible (and much easier), calibration methods that are synergistically using both measurements (Chla fluorescence and radiometry) can be developed (e.g., Xing et al. 2011). These methods are based on robust global bio-optical relationships that allow establishing calibration coefficients that are pertinent over the platform lifetime (Xing et al. 2011).

The second important issue concerns the coherence of data sets acquired by different elephant seals and their associated fluorometers. Cross-calibration of fluorometers here appears the only way to guarantee this coherence. This is well evidenced by the variability of the calibration coefficients derived from in situ measurements, which again highlights the relative weaknesses of factory calibration (Table 2, Fig. 1). This coherence is obviously restricted to a calibration series (three series were performed at different period for all fluorometers concerned here). Furthermore this dataset coherence requires the rather reasonable assumption that, once deployed, all fluorometers evolve similarly over the acquisition time.

Note that the method proposed by Xing et al. (2011) relying on global bio-optical relationship is also a way to guarantee a coherence of the Chl *a* database through different fluorometers carried by different platforms. Recently a method was also proposed (Lavigne et al. 2012) to make use of the Chl *a* concentration remotely detected through ocean color satellite as a reference value for establishing a calibration factor for the fluorescence profile co-located with the satellite measurement. In such a way all profiles acquired by different platforms have a common reference, the satellite Chl *a*. The method proposed by Lavigne et al. (2012) makes use of the quenching correction proposed here. Finally other methods have been proposed (Mignot et al. 2011) to infer the profile of Chl *a* concentration from the sole knowledge of the shape of the fluorescence profile. These methods are designed for global scale applications but are not recommended for regional or local applications.

The last issue is directly linked to the specificity of fluorescence measurement and to the so-called NPQ. This well-recognized phenomenon obviously generates a significant and variable bias in the retrieval of "accurate" Chl *a* concentration and consequently generates "noise" in large databases. To cope with this issue, one first and easy solution is to keep only the night measurements in the datasets. This would

obviously eliminate possibly interesting data, thus lowering the spatial and/or temporal resolution of the measurements. In the present case, this would definitively preclude any interpretation at potentially interesting scales (sub-mesoscale, mesoscale) along the seal transect. For some other scientific application, accurate Chl *a* concentration estimations are required (mandatory) in the daytime (or specifically at noon); this is the case for sea truths of ocean color satellite (validation dataset). Correction schemes for getting the most accurate Chl *a* concentration from fluorimetric profile are thus required. For multi-instrumented platforms like glider embarking both fluorometers and backscattering sensors, Sackmann et al. (2008) proposed an elegant method that made use of the backscattering profile to correct the fluorimetric one. However, there is still no solid proof to support their assumption that the particle backscattering coefficient is regularly associated with Chl *a* concentrations. In the present case with no synchronous measurement other than the temperature/salinity profiles, we assume that the vertical distribution of all phytoplankton properties was homogenous in the mixed layer, somewhat robustly but practically.

This correction scheme was tested at the Boussole site, and an improvement of the [Chl *a*] retrieval by ~10% was shown above (the MAPE is improved from 39% to 29%). At this stage, the only concerns and limit of the approach proposed here can be when the biological properties (i.e., the Chl *a* biomass itself) are paradoxically not mixed within the so-called mixed layer. This (potentially rare) case are likely at the origin of the subtle distinction between mixed and mixing layers, a concept recently re-introduced by Taylor and Ferrari (2011). This peculiar situation might occur when temporary reduction of surface turbulence allows biomass development in the upper part of a "mixed" layer (Taylor and Ferrari 2011).

Comments and recommendations

Instrumented animals allow oceanic observations in remote and harsh areas. As for any other kind of autonomous platforms (e.g., gliders, profiling floats), sensor calibration and validation, and eventual correction of measured variables remain important challenges.

Based on our observations and analyses, the fluorescence quenching is a very significant issue when dealing with the accurate retrieval of [Chl *a*] from fluorescence measurements. The difference between day and night surface profiles of fluorescence is not related to any associated changes of Chl *a*. Without any quenching correction scheme, the diel variation of in vivo fluorescence at surface could be responsible for a significant underestimation of Chl *a* concentration and possibly of derived variables or rates (phytoplankton biomass and primary productivity).

In this study, we presented and discussed a possible correction for this quenching problem, with the assumption of quasi-homogeneity of chlorophyll concentration in the mixed layer. It is especially adapted when there are not alternate or companion measurements to help in this correction, which is often the case in the remote areas of the Southern Ocean.

Acknowledgments

This paper represents a contribution to the ANR VMC 2007-IPSOS-SEAL (Investigation of the vulnerability of the biological Productivity of the Southern Ocean Subsystems to climate change: the Southern Elephant seal Assessment from mid to high Latitudes) project. This program was financially supported by the CNES-TOSCA (Elephant seals as oceanographer: fluorescence measurements) and was conducted as part of the program 109 (resp. H. Weimerskirch) of the French Polar Institute Paul Emile Victor. This paper was also funded by the China Postdoctoral Science Foundation funded project (2012M511065), the Hong Kong General Grant Fund (GRF) (CUHK454909 & CUHK459210) and ITF (ITS/058/09FP). We wish to thank all the people involved in the field work and the BOUSSOLE program for its continuous support in the field testing of the CTD-Fluo tag in the Mediterranean Sea prior to their deployment on elephant seals. Special thanks to Emily Walker and Stéphane Marchand who contributed greatly to the management of the fluorescence data collected. At last, we express our gratitude to Heidi Sosik for helpful suggestions and constructive comments on a first version of this paper.

References

Antoine, D., F. D'Ortenzio, S. B. Hooker, G. Bécu, B. Gentili, D. Tailliez, and A. J. Scott. 2008. Assessment of uncertainty in the ocean reflectance determined by three satellite ocean color sensors (MERIS, SeaWiFS, and MODIS-A) at an offshore site in the Mediterranean Sea. J. Geophys. Res. 113:C07013 [doi:101029/102007JC004472].

Babin, M. 2008. Phytoplankton fluorescence: theory, current literature, and in situ measurements, p. 237-280. *In* M. Babin, C. Roesler, and J. J. Cullen [eds.], Real-time coastal observing systems for marine ecosystem dynamics and harmful algal blooms. Unesco.

———, A. Morel, and B. Gentili. 1996. Remote sensing of sea surface sun-induced chlorophyll fluorescence: Consequences of natural variations in the optical characteristics of phytoplankton and the quantum yield of chlorophyll a fluorescence. Int. J. Remote Sens. 17:2417-2448 [doi:10.1080/01431169608948781].

Behrenfeld, M. J., and E. Boss. 2006. Beam attenuation and chlorophyll concentration as alternative optical indices of phytoplankton biomass. J. Mar. Res. 64:431-451 [doi:10.1357/002224006778189563].

Biuw, M., and others. 2007. Variations in behaviour and condition of a Southern Ocean top predator in relation to in-situ oceanographic conditions. Proc. Natl. Acad. Sci. 104:13705-13710 [doi:10.1073/pnas.0701121104].

Blain, S., B. Quéguiner, and T. Trull. 2008. The natural iron fertilization experiment KEOPS (KErguelen Ocean and Plateau compared Study): An overview. Deep-Sea Res. II 55:559-565

[doi:10.1016/j.dsr2.2008.01.002].

Charrassin, J. B., and others. 2008. Southern ocean frontal structure and sea-ice formation rates revealed by elephant seals. Proc. Natl. Acad. Sci. 105:11634-11639 [doi:10.1073/pnas.0800790105].

Claustre, H., and others. 2010. Bio-optical profiling floats as new observational tools for biogeochemical and ecosystem studies: potential synergies with ocean color remote sensing. *In* J. Hall, D. E. Harrison, and D. Stammer (Eds.), Proceedings of OceanObs'09: Sustained ocean observations and information for society (Vol. 2), Venice, Italy, 21-25 September 2009. ESA Publication WPP-306 [doi:10.5270/OceanObs09.cwp.17].

Cullen, J. J., and M. R. Lewis. 1995. Biological processes and optical measurements near the sea-surface: some issues relevant to remote sensing. J. Geophys. Res. 100(C7):13255-13266 [doi:10.1029/95JC00454].

de Boyer Montégut, C., G. Madec, A. S. Fischer, A. Lazar, and D. Iudicone. 2004. Mixed layer depth over the global ocean: an examination of profile data and a profile-based climatology. J. Geophys. Res. 109: C12003 [doi:10.1029/2004JC002378].

Falkowski, P. G., and Z. Kolber. 1995. Variations in chlorophyll fluorescence yields in phytoplankton in the world oceans. Aust. J. Plant Physiol. 22:341-355 [doi:10.1071/PP9950341].

Fedak, M. 2004. Marine animals as platforms for oceanographic sampling: A "win/win_' situation for biology and operational oceanography. Mem. Nat. Inst. Polar Res. 58:133-147.

Field, I. C., C. J. Bradshaw, C. R. McMahon, J. Harrington, and H. R. Burton. 2002. Effects of age, size and condition of elephant seals (Mirounga leonina) on their intravenous anaesthesia with tiletamine and zolazepam. Vet. Rec. 151:235-240 [doi:10.1136/vr.151.8.235].

Holm-Hansen, O., A. F. Amos, and C. D. Hewes. 2000. Reliability of estimating chlorophyll-a concentrations in Antarctic waters by measurement of in situ chlorophyll-a fluorescence. Mar. Ecol. Progr. Ser. 196:103-110 [doi:10.3354/meps196103].

Johnson, K. S., and others. 2009. Observing biogeochemical cycles at global scales with profiling floats and gliders: prospects for a global array. Oceanography 22:216-225 [doi:10.5670/oceanog.2009.81].

Kiefer, D. A. 1973. Fluoresence properties of natural phytoplankton populations. Mar. Biol. 22:263-269 [doi:10.1007/BF00389180].

Krause, G. H., and E. Weis. 1991. Chlorophyll fluorescence and photosynthesis: The basics. Annu. Rev. Plant Physiol. 42:313-349 [doi:10.1146/annurev.pp.42.060191.001525].

Lavigne, H., F. D'Ortenzio, H. Claustre and A. Poteau. 2011. Towards a merged satellite and in situ fluorescence ocean chlorophyll product. Biogeosci. Discuss. 8:11899-11939 [doi:10.5194/bgd-8-11899-2011].

Lorenzen, C. 1966. A method for the continuous measurement of in vivo chlorophyll concentration. Deep-Sea Res. 13:223-227.

Marra, J. 1997. Analysis of diel variability in chlorophyll fluorescence. J. Mar. Res. 55:767-784 [doi:10.1357/0022240973224274].

Maxwell, K., and G. N. Johnson. 2000. Chlorophyll fluorescence—a practical guide. J. Exp. Bot. 51:659-668 [doi:10.1093/jexbot/51.345.659].

Mignot, A., H. Claustre, F. D'Ortenzio, X. Xing, A. Poteau, and J. Ras. 2011. From the shape of the vertical profile of in vivo fluorescence to chlorophyll-a concentration. Biogeosciences 8:2391-2406 [doi:10.5194/bg-8-2391-2011].

Morrison, J. R. 2003. In situ determination of the quantum yield of phytoplankton chlorophyll a fluorescence: A simple algorithm, observations, and a model. Limnol. Oceanogr. 48:618-631 [doi:10.4319/lo.2003.48.2.0618].

Ras, J., H. Claustre, and J. Uitz. 2008. Spatial variability of phytoplankton pigment distributions in the Subtropical South Pacific Ocean: comparison between in situ and predicted data. Biogeosciences 5:353-369 [doi:10.5194/bg-5-353-2008].

Roquet, F., J. B. Charrassin, S. Marchand, L. Boehme, M. Fedak, G. Reverdin, and C. Guinet. 2011. Validation of hydrographic data obtained from animal-borne satellite-relay data loggers. J. Atmos. Ocean Technol. 28:787-801 [doi:10.1175/2010JTECHO801.1].

Sackmann, B. S., M. J. Perry, and C. C. Eriksen. 2008. Seaglider observations of variability in daytime fluorescence quenching of chlorophyll-a in Northeastern Pacific coastal waters. Biogeosci. Discuss. 5:2839-2865 [doi:10.5194/bgd-5-2839-2008].

Serra, T., C. Borrego, X. Quintana, L. Calderer, R. López, and J. Colomer. 2009. Quantification of the effect of nonphotochemical quenching on the determination of in vivo Chl a from phytoplankton along the water column of a freshwater reservoir. Photochem. Photobiol. 85:321-331 [doi:10.1111/j.1751-1097.2008.00441.x].

Schallenberg, C., M. R. Lewis, D. E. Kelley and J. J. Cullen. 2008. Inferred influence of nutrient availability on the relationship between Sun-induced chlorophyll fluorescence and incident irradiance in the Bering Sea. J. Geophys. Res. 113:C07046 [doi:10.1029/2007JC004355].

Taylor, J. R., and R. Ferrari. 2011. Shutdown of turbulent convection as a new criterion for the onset of spring phytoplankton blooms. Limnol. Oceanogr. 56(6):2293-2307 [doi:10.4319/lo.2011.56.6.2293].

Uitz, J., H. Claustre, N. Garcia, F.B. Griffiths, J. Ras and V. Sandroni. 2009. A phytoplankton class-specific primary production model applied to the Kerguelen Islands region (Southern Ocean). Deep-Sea Res. I 56:541–560 [doi:10.1016/j.dsr.2008.11.006].

Xing, X., A. Morel, H. Claustre, D. Antoine, F. D'Ortenzio, A. Poteau, and A. Mignot. 2011. Combined processing and

mutual interpretation of radiometry and fluorimetry from autonomous profiling Bio-Argo Floats: Chlorophyll a retrieval. J. Geophys. Res. 116:C06020 [doi:10.1029/2010JC006899].

Submitted 19 August 2011
Revised 6 April 2012
Accepted 19 April 2012